ISSN 1070-3284, Russian Journal of Coordination Chemistry, 2022, Vol. 48, No. 12, pp. 772–783. © Pleiades Publishing, Ltd., 2022.
Russian Text © The Author(s), 2022, published in Koordinatsionnaya Khimiya, 2022, Vol. 48, No. 12, pp. 718–729.

Copper(II) Complexes with CF_3-Substituted Spin-Labeled Pyrazoles

A. S. Bogomyakov[a], *, G. V. Romanenko[a], S. V. Fokin[a], E. T. Chubakova[a], E. V. Tretyakov[b], and V. I. Ovcharenko[a]

[a] *International Tomography Center, Siberian Branch, Russian Academy of Sciences, Novosibirsk, 630090 Russia*

[b] *Zelinsky Institute of Organic Chemistry, Russian Academy of Sciences, Moscow, 119991 Russia*

**e-mail: bus@tomo.nsc.ru*

Received June 22, 2022; revised July 6, 2022; accepted July 6, 2022

Abstract—CF_3-substituted pyrazolyl nitroxides L^{R/CF_3} and their Cu(II) complexes were synthesized. The molecular and crystal structures of the products were studied by X-ray diffraction (CCDC no. 2180506–2180521). It was found that the introduction of the electron-withdrawing CF_3 group into the pyrazole ring decreases the donor ability of the N atom, and nitronyl nitroxides L^{R/CF_3} are coordinated in heterospin complexes only by the O atoms of the nitronyl nitroxide moieties. Magnetochemical studies of polymer chain complexes $[Cu(Hfac)_2L^{R/CF_3}]_n$ (Hfac = hexafluoroacetylacetonate anion) in the 2–300 K range revealed ferromagnetic ordering at temperatures below 5 K. Thermally induced magnetic structural phase transitions were detected in two polymorphs of the molecular complex, α-$[Cu(Hfac)_2\left(L^{Me/CF_3}\right)_2]$ and β-$[Cu(Hfac)_2\left(L^{Me/CF_3}\right)_2]$. These polymorphs are new examples of molecular heterospin complexes that undergo thermally induced magnetic structural phase transitions without crystal degradation.

Keywords: nitronyl nitroxides, pyrazoles, copper complexes, heterospin complexes, molecular ferromagnets
DOI: 10.1134/S1070328422700014

INTRODUCTION

Systematic studies of the crystals based on polymer chain heterospin complexes of bis(hexafluoroacetylacetonato)copper $Cu(Hfac)_2$ with spin-labeled alkyl-substituted pyrazoles (L^R) (Scheme 1), $[Cu(Hfac)_2L^R]$ and their solvates $[Cu(Hfac)_2L^R]\cdot x$Solv, resulted in detection of a variety of magnetic anomalies in thermomagnetic curves, inherent in the nature of this class of compounds [1–5]. It was ascertained that the observed anomalies are sensitive to even minor changes in the molecular packing [3, 5]. Similar magnetic effects were also found for multispin compounds $[Cu(Hfac)_2L^{R/R'}]$ with dialkyl-substituted pyrazoles ($L^{R/R'}$) (Scheme 1), studies of which not only substantially extended the range of magnetically active compounds, but also revealed complexes that undergo reversible topochemical reactions in the crystals upon temperature change, such as polymerization–depolymerization and depolymerization–polymerization reactions (single crystal to single crystal transformations, SC ↔ SC), accompanied by hysteresis effects in the curves for temperature dependence of effective magnetic moment (μ_{eff}) [6–8]. Also, acyclic oligomeric molecular Cu(II) complexes with spin-labeled pyrazoles of unusual 5 : 4 composition and cyclic binuclear complexes able to undergo spin transitions were reported [9].

Since the presence of fluorinated components is a favorable factor for the appearance of mechanical activity in the crystals [10], we made an attempt to prepare and study heterospin complexes containing, in addition to stereochemically non-rigid fluorinated acceptor matrix $[Cu(Hfac)_2]$, also a fluorinated spin-labeled pyrazole derivative $\left(L^{R/CF_3}\right)$ (Scheme 1).

In this study, we describe the synthesis of nitronyl nitroxides L^{R/CF_3}, and $Cu(Hfac)_2$ complexes with these radicals and the results of studying the structure and magnetic properties of the obtained compounds.

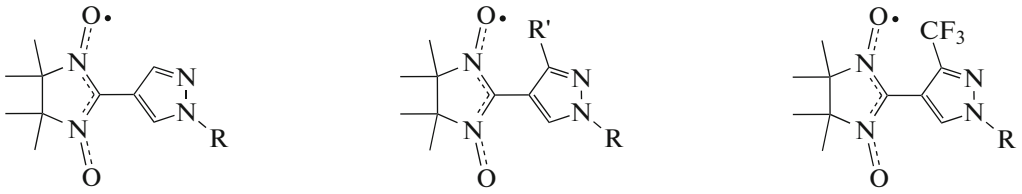

L^R R = Me, Et, *n*-Pr, *i*-Pr, *n*-Bu

$L^{R/R'}$ R, R' = Me, Et, *n*-Pr, *n*-Bu

L^{R/CF_3} R = Me, Et, *n*-Pr

Scheme 1.

EXPERIMENTAL

2,3-Bis(hydroxyamino)-2,3-dimethylbutane sulfate hydrate [11] and 4-formyl-3-trifluoromethyl-1*H*-pyrazole [12] were synthesized by reported procedures. Commercial reactants and solvents were used as received. TLC was carried out on Silica Gel 60 F_{254} plates with a sorbent layer attached to aluminum foil. Column chromatography was conducted using silica gel with 0.063–0.200 mm pellets (Merck). Elemental analysis was performed on a Euro EA 3000 microanalyzer. IR spectra of the sample in KBr pellets were recorded on a Bruker Vector-22 spectrophotometer.

Synthesis of 2-(3-trifluoromethyl-1*H*-pyrazol-4-yl)-4,4,5,5-tetramethyl-4,5-dihydro-1*H*-imidazole-1-oxyl 3 oxide (L^{H/CF_3}). A solution of 2,3-bis-hydroxylamino-2,3-dimethylbutane sulfate hydrate (1.30 g, 4.8 mmol) in water (13 mL) was added to 4-formyl-3-trifluoromethyl-1*H*-pyrazole (0.67 g, 4.0 mmol), and the reaction mixture was stirred for 2 h and treated with $NaHCO_3$ until CO_2 evolution stopped. The resulting 2-(3-trifluoromethyl-1*H*-pyrazol-4-yl)-4,4,5,5-tetramethylimidazolidine-1,3-diol (diol) was collected on a filter, washed with water and acetone, dried, and recrystallized from a EtOAc and hexane mixture (3 : 1). The yield was 0.85 g (74%). MnO_2 (4.2 g, 49 mmol) was added in portions over a period of 10 min to a stirred solution of diol (0.85 g, 2.9 mmol) in CH_3OH (18 mL), then the reaction mixture was stirred for 1.5 h at room temperature and filtered. The precipitate was washed with CH_3OH. The filtrate was concentrated, and the residue was chromatographed on a column with silica gel (1.5 × 15 cm). The turquoise-colored fraction, which came out first, was evaporated, and the residue was crystallized from a mixture of ether and hexane to give the nitroso derivative, *N*-(2,3-dimethyl-3-nitrosobutan-2-yl)-1-(3-(trifluoromethyl)-1H-pyrazol-4-yl)metanimine oxide (L*) (Scheme 2), which was studied by X-ray diffraction. The yield was 44 mg (5.3%), T_m = 134–135°C.

IR (ν, cm^{-1}): 3130, 3072, 2998, 2924, 2361, 1604, 1563, 1480, 1396, 1369, 1321, 1259, 1182, 1127, 1062, 937, 919, 838, 759, 724, 669, 636.

For $C_{11}H_{14}N_4O_2F_3$

Anal. calcd., %	C, 45.4	H, 4.8	N, 19.2	F, 19.6
Found, %	C, 45.3	H, 4.5	N, 19.2	F, 20.2

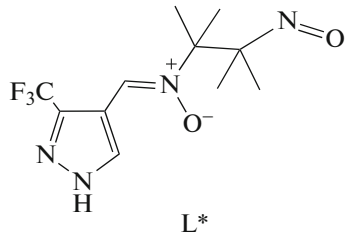

L*

Scheme 2.

The second violet-colored fraction was also evaporated to give nitroxide L^{H/CF_3}. The yield was 770 mg, 91%, T_m = 182–183°C (ether–hexane).

IR (ν, cm^{-1}): 3113, 2990, 2362, 1597, 1510, 1460, 1403, 1359, 1279, 1222, 1169, 1122, 1083, 1051, 940, 805, 739, 649.

For $C_{11}H_{14}F_3N_4O_2$

Anal. calcd., %	C, 45.4	H, 4.8	N, 19.2	F, 19.6
Found, %	C, 44.9	H, 5.1	N, 19.4	F, 19.4

Synthesis of 2-(1-methyl-3-trifluoromethyl-1*H*-pyrazol-4-yl)-4,4,5,5-tetramethyl-4,5-dihydro-1*H*-imidazol-1-oxyl 3-oxide (L^{Me/CF_3}). NaH (60% in mineral oil, 34 mg, 0.86 mmol) was added under argon with stirring at room temperature to a solution of L^{H/CF_3} (245 mg, 0.86 mmol) in DMF (3 mL). The reaction mixture was stirred for 30 min, dimethyl sulfate (102 μL, 1.0 mmol) was added, and the mixture was stirred for an additional 30 min. The solvent was evaporated in vacuum at ~70°C temperature of the

bath, the residue was chromatographed on a column with silica gel (1.5 × 18 cm), and the product was eluted with ethyl acetate. The violet fraction was concentrated and the residue was crystallized from a CH_2Cl_2 and hexane mixture (1 : 5). The yield was 160 mg (62%), T_m = 110–111°C.

IR (ν, cm^{-1}): 3139, 3034, 2993, 2947, 1597, 1498, 1480, 1457, 1412, 1399, 1375, 1359, 1306, 1285, 1243, 1222, 1070, 1151, 1136, 1080, 1059, 1020, 870, 838, 768, 739, 645, 616, 588.

For $C_{12}H_{16}N_4O_2F_3$

Anal. calcd., %	C, 47.2	H, 5.3	N, 18.3	F, 18.7
Found, %	C, 46.7	H, 5.1	N, 18.1	F, 18.4

Synthesis of 2-(1-ethyl-3-trifluoromethyl-1*H*-pyrazol-4-yl)-4,4,5,5-tetramethyl-4,5-dihydro-1*H*-imidazol-1-oxyl 3-oxide (L^{Et/CF_3}) was carried out by a similar procedure from EtBr (0.11 mL, 1.4 mmol). The yield was 0.19 g (85%), T_m = 128–129°C.

IR (ν, cm^{-1}): 3095, 2985, 2944, 1604, 1508, 1484, 1452, 1404, 1371, 1324, 1251, 1238, 1176, 1129, 1106, 1089, 1062, 1025, 962, 861, 828, 767, 741, 656.

For $C_{13}H_{18}F_3N_4O_2$

Anal. calcd., %	C, 48.9	H, 5.7	N, 17.5	F, 17.8
Found, %	C, 48.5	H, 5.3	N, 17.5	F, 18.2

Synthesis of 2-(1-propyl-3-trifluoromethyl-1*H*-pyrazol-4-yl)-4,4,5,5-tetramethyl-4,5-dihydro-1*H*-imidazol-1-oxyl 3-oxide (L^{Pr/CF_3}) was carried out by a similar procedure from PrBr (0.073 mL, 0.80 mmol). The yield was 0.15 g (82%), T_m = 106–107°C.

IR (ν, cm^{-1}): 3126, 2990, 2943, 2878, 1604, 1509, 1490, 1450, 1406, 1370, 1327, 1281, 1240, 1220, 1143, 1061, 1017, 901, 863, 831, 741, 653.

For $C_{14}H_{20}N_4O_2F_3$

Anal. calcd., %	C, 50.4	H, 6.0	N, 16.8	F, 17.1
Found, %	C, 50.4	H, 5.3	N, 17.1	F, 18.2

Synthesis of $[Cu(Hfac)_2L^{Me/CF_3}]_n$ (I). A solution of $Cu(Hfac)_2$ (0.0477 g, 0.1 mmol) in hexane (2 mL) was added to a solution of L^{Me/CF_3} (0.0300 g, 0.1 mmol) in CH_2Cl_2 (2 mL), and the reaction mixture acquired an intense brown-red color. The reaction mixture was kept at –18°C for ~130 h. The resulting prismatic dark brown crystals were collected on a filter, washed with cooled hexane, and dried in air. The yield was 0.070 g (90%).

For $C_{22}H_{18}N_4O_6F_{15}Cu$

Anal. calcd., %	C, 33.7	H, 2.3	N, 7.2	F, 36.4
Found, %	C, 33.2	H, 2.8	N, 7.3	F, 36.3

Synthesis of $[Cu(Hfac)_2L^{Et/CF_3}]_n$ (II). A mixture of $Cu(Hfac)_2$ (0.0674 g, 0.14 mmol) and L^{Et/CF_3} (0.0313 g, 0.1 mmol) was dissolved in toluene (2 mL). A part of the solvent was slowly stripped with an air flow to a volume of ~1 mL, then the reaction mixture was kept at –18°C for 40 h. Brown-colored crystals were collected on a filter, washed with cooled hexane, and dried in air. The yield was 0.039 g (50%).

For $C_{23}H_{20}N_4O_6F_{15}Cu$

Anal. calcd., %	C, 34.7	H, 2.5	N, 7.0	F, 35.8
Found, %	C, 35.1	H, 2.7	N, 6.7	F, 35.7

Synthesis of $[Cu(Hfac)_2L^{Pr/CF_3}]_n$ (III). A mixture of $Cu(Hfac)_2$ (0.0472 g, 0.1 mmol) and L^{Pr/CF_3} (0.0301 g, 0.1 mmol) was dissolved in hexane (4 mL). Some of the solvent was slowly stripped with an air flow to a volume of ~1 mL, the solution was kept at –18°C for 48 h. Brown-colored crystals were collected on a filter, washed with cooled hexane, and dried in air. The yield was 0.028 g (36%).

For $C_{24}H_{22}CuF_{15}N_4O_6$

Anal. calcd., %	C, 35.5	H, 2.7	N, 6.9	F, 35.1
Found, %	C, 35.6	H, 2.6	N, 7.0	F, 35.3

Synthesis of α-$[Cu(Hfac)_2(L^{Me/CF_3})_2]$ (IV). A weighed amount of $Cu(Hfac)_2$ (0.0300 g, 0.06 mmol) was dissolved in Et_2O (1.5 mL). A weighed amount of L^{Me/CF_3} (0.0200 g, 0.07 mmol) was dissolved in Et_2O (3 mL). The solution of $Cu(Hfac)_2$ was added to a solution of L^{Me/CF_3}; the reaction mixture acquired an intense red-brown color. After thorough mixing, toluene (2 mL) was added, and the mixture was kept at –18°C for ~17 days. The dark burgundy-colored crystals were collected on a filter, washed with cooled hexane, and dried in air. The yield was 0.014 g (39%). T_m = 116–117°C.

For $C_{34}H_{34}N_8O_8F_{18}Cu$

Anal. calcd., %	C, 37.5	H, 3.1	N, 10.3	F, 31.4
Found, %	C, 39.2	H, 3.2	N, 10.4	F, 30.6

Table 1. Crystallographic data and X-ray experiment and structure refinement details for nitroxides L^{R/CF_3}

Parameter	Nitroxide					
	L^{H/CF_3}	L^{Me/CF_3}-a	L^{Me/CF_3}-b	L^{Me/CF_3}-c	L^{Et/CF_3}	L^{Pr/CF_3}
M	291.26	305.29			319.32	333.34
T, K	296	296			296	296
Space group, Z	$P2_1/c$, 4	$P\bar{1}$, 2	$P2_1/c$, 4	$P2_1/c$, 8	$P2_1/c$, 4	$P2_1/c$, 8
a, Å	10.3659(9)	7.4217(7)	10.2998(11)	7.1341(14)	10.492(4)	7.7542(11)
b, Å	10.1986(8)	10.1430(10)	20.745(2)	11.872(2)	13.397(5)	17.776(2)
c, Å	13.1267(13)	10.1759(9)	7.2967(8)	35.062(7)	11.253(4)	12.2262(18)
α, deg		93.043(6)				
β, deg	110.696(6)	100.238(6)	102.072(7)	90.00(3)	100.50(3)	90.998(12)
γ, deg		107.590(6)				
V, Å^3	1298.2(2)	713.91(12)	1524.6(3)	2969.6(10)	1555.3(10)	1685.0(4)
ρ(calcd.) g/cm^3	1.490	1.420	1.330	1.366	1.364	1.314
θ_{max}, deg	45.234	28.335	66.075	23.245	28.502	28.409
I_{hkl} measured/unique	3798/1061	11870/3519	7619/2459	7124/2617	13771/3850	15197/4176
R_{int}	0.042	0.0491	0.0308	0.0341	0.1168	0.1697
I_{hkl} observed ($I > 2\sigma(I)$)/N	921/186	1765/195	2201/218	1900/488	882/227	1054/208
GOOF	1.027	0.916	1.026	0.989	0.645	0.971
R_1/wR_2 ($I > 2\sigma(I)$)	0.0358/0.0816	0.0404/0.0944	0.0515/0.1520	0.0546/0.1469	0.0425/0.0661	0.0741/0.1296
R_1/wR_2	0.0539/0.0905	0.0928/0.1085	0.0555/0.1570	0.0724/0.1596	0.2624/0.0918	0.3133/0.1894
CCDC	2180506	2180509	2180516	2180511	2180520	2180519

Synthesis of β-[Cu(Hfac)$_2$(L^{Me/CF_3})$_2$] (V). A mixture of weighed amounts of Cu(Hfac)$_2$ (0.0318 g, 0.07 mmol) and L^{Me/CF_3} (0.0400 g, 0.13 mmol) was dissolved in toluene (2 mL). The reaction mixture was vigorously stirred, then the resulting solution was kept at −30°C for ~20 days. The crystals thus formed were collected on a filter, washed with cooled hexane, and dried in air. The yield was 0.008 g (11%).

X-ray diffraction. The sets of reflections from single crystals were collected on a Bruker AXS—SMART APEX automated diffractometer (MoK_α radiation) with a Helix open flow helium cooler (Oxford Cryosystems) and an Apex Duo automated diffractometer (CuK_α radiation) with a Cobra cryogenic system (Oxford Cryosystems) by a standard procedure. The structures were solved by direct methods and refined by the full matrix least squares method in the anisotropic approximation for non-hydrogen atoms. Some H atoms were located from difference electron density maps (the other H atoms were calculated geometrically) and included in the refinement in the riding model. All calculations were performed using the SHELX software package [13]. The crystallographic characteristics of the compounds and X-ray experiment details are summarized in Tables 1–3.

The full sets of X-ray diffraction data were deposited with the Cambridge Crystallographic Data Centre (no. 2180506–2180521, http://www.ccdc.cam.ac.uk).

Magnetic measurements were carried out on a MPMSXL SQUID magnetometer (Quantum Design) in the temperature range of 2–300 K in a magnetic field of up to 5 kOe. The paramagnetic components of the magnetic susceptibility (χ) were determined taking account of the diamagnetic contribution estimated by the Pascal scheme. The effective magnetic moment (μ_{eff}) was calculated by the formula $\mu_{eff} = [3k\chi T/(N_A\mu_B^2)]^{1/2} \approx (8\chi T)^{1/2}$, where N_A, μ_B, and k are the Avogadro number, the Bohr magneton, and the Boltzmann constant, respectively.

Table 2. Crystallographic data and X-ray experiment and structure refinement details for L* and **I–III**

Parameter	Compound			
	L*	$[Cu(Hfac)_2L^{Me/CF_3}]$ (**I**)	$[Cu(Hfac)_2L^{Et/CF_3}]$ (**II**)	$[Cu(Hfac)_2L^{Pr/CF_3}]$ (**III**)
M	292.27	782.94	796.97	810.99
T, K	296	296	296	296
Space group, Z	$P2_1/c$, 4	$P\bar{1}$, 2	$Pbca$, 8	$Pbca$, 8
a, Å	9.552(2)	10.2987(5)	19.0454(5)	18.878(4)
b, Å	10.951(3)	12.4776(6)	16.0497(5)	16.199(4)
c, Å	13.308(4)	13.0064(6)	20.6628(6)	21.179(5)
α, deg	100.27(2)	80.128(2)	90	90
β, deg		84.107(2)	90	90
γ, deg		69.199(2)	90	90
V, Å^3	1369.8(6)	1537.70(13)	6316.1(3)	6477(3)
ρ(calcd.), g/cm^3	1.417	1.691	1.676	1.663
θ_{max}, deg	28.371	28.469	55.696	45.211
I_{hkl} measured/unique	12379/3409	17865/6995	36473/4031	51137/2626
R_{int}	0.0584	0.0563	0.0921	0.1062
I_{hkl} observed $(I > 2\sigma(I))/N$	1163/237	3038/536	2884/595	1643/452
GOOF	0.721	1.013	0.867	1.027
R_1/wR_2 $(I > 2\sigma(I))$	0.0398/0.0782	0.0524/0.1084	0.0385/0.0966	0.0689/0.1779
R_1/wR_2	0.1452/0.1020	0.1483/0.1412	0.0569/0.1050	0.1151/0.2182
CCDC	2180507	2180510	2180512	2180517

RESULTS AND DISCUSSION

The synthesis of 2-(1-*R*-3-trifluoromethyl-1*H*-pyrazol-4-yl)-4,4,5,5-tetramethyl-4,5-dihydro-1*H*-imidazol-1-oxyl 3-oxides $\left(L^{R/CF_3}\right)$ included the condensation of 4-formyl-3-trifluoromethyl-1*H*-pyrazole with bis(hydroxylamine), resulting in the formation of dihydroxy derivative, oxidation of the product to nitronyl nitroxide L^{H/CF_3}, and subsequent alkylation of L^{H/CF_3} (Scheme 3).

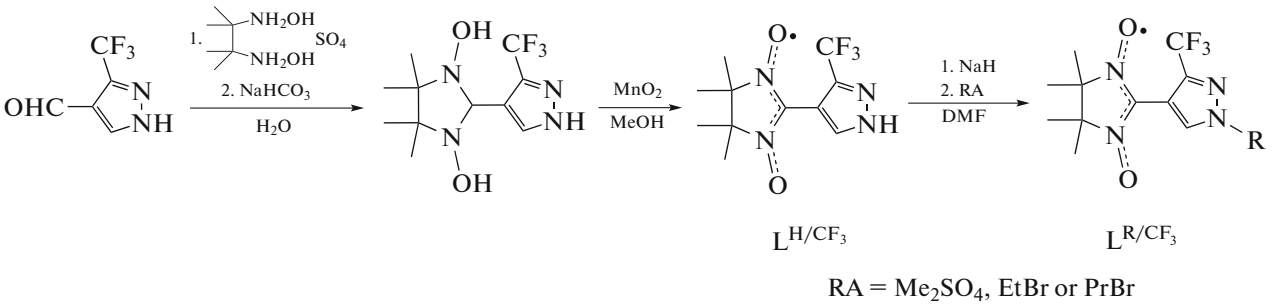

Scheme 3.

The alkylation of substituted pyrazole L^{H/CF_3} was regioselective and gave only one isomer in which the CF_3 group was located in position 3 of the aromatic ring. This is indicated by the single crystal X-ray dif-

Table 3. Crystallographic data and X-ray experiment and structure refinement details for **IV** and **V**

Parameter	Complex					
	α-[Cu(Hfac)$_2$(L$^{Me/F_3}$)$_2$] (**IV**)		β-[Cu(Hfac)$_2$(L$^{Me/F_3}$)$_2$] (**V**)			
M	1088.23		1088.23			
T, K	296	120	296	240	150	120
Space group, Z	$P\bar{1}$, 2		$P\bar{1}$, 2			
a, Å	10.3895(2)	10.3149(3)	9.9143(13)	9.8761(5)	9.8143(3)	9.8144(3)
b, Å	10.7909(2)	10.5119(3)	10.3735(13)	10.3715(5)	10.3698(3)	10.3851(6)
c, Å	12.1712(2)	12.0415(3)	12.4117(17)	12.3466(6)	12.2101(3)	12.1083(4)
α, deg	114.9670(10)	114.6410(10)	71.403(9)	71.292(3)	71.068(2)	103.196(3)
β, deg	95.5240(10)	96.652(2)	68.312(8)	67.635(3)	66.787(2)	113.618(2)
γ, deg	107.4420(10)	107.010(2)	82.932(9)	82.894(3)	82.912(2)	97.311(3)
V, Å^3	1140.32(4)	1091.54(5)	1124.2(3)	1107.74(10)	1080.26(6)	1067.29(8)
ρ(calcd.), g/cm^3	1.585	1.656	1.607	1.631	1.673	1.693
θ_{max}, deg	28.028	28.484	51.763	28.534	28.404	28.368
I_{hkl} measured/unique	19717/5494	19535/5394	10752/2352	18983/5450	17944/5296	18246/5264
R_{int}	0.0501	0.0711	0.0318	0.0500	0.0760	0.0920
I_{hkl} observed ($I > 2\sigma(I)$)/N	3749/385	4018/386	2055/367	3256/367	2980/368	2516/342
GOOF	0.953	0.894	1.037	0.925	0.841	0.863
R_1/wR_2 ($I > 2\sigma(I)$)	0.0356/0.0879	0.0378/0.0885	0.0376/0.1028	0.0402/0.0929	0.0429/0.0772	0.0473/0.0947
R_1/wR_2	0.0579/0.0954	0.0564/0.0950	0.0425/0.1071	0.0792/0.1031	0.0849/0.0865	0.7782/0.1231
CCDC	2180508	2180521	2180518	2180515	2180514	2180513

fraction data for L$^{R/CF_3}$. The N–O bond lengths in all L$^{R/CF_3}$ are in the 1.273(4)–1.289(4) Å range, typical of nitronyl nitroxide radicals [14]. In the structure of L$^{H/CF_3}$, unlike L$^{R/CF_3}$, the molecules form chains due to H-bonds between the pyrazole imine group and one O_{NO} atom (Fig. 1). For L$^{Me/CF_3}$, three polymorphs were found (L$^{Me/CF_3}$-a–c), in which the molecules differ in the angles between the planes of the pyrazole ring and the {CN_2O_2} paramagnetic moiety (Table 4), in the molecular packing, and in the type of intermolecular contacts (Fig. 2). The shortest distances between the paramagnetic centers, the O_{NO} atoms of neighboring molecules, exceed 3.5 Å in all L$^{R/CF_3}$.

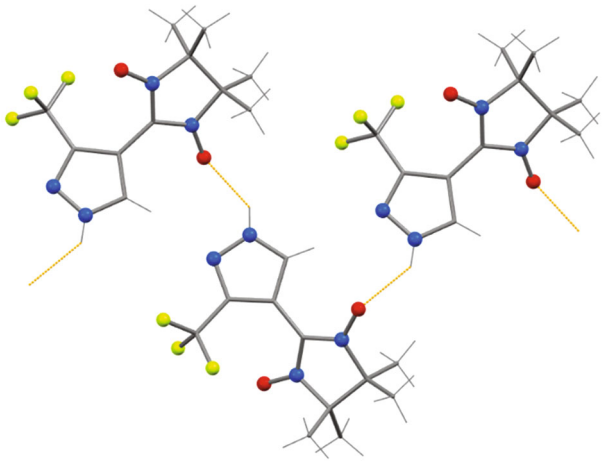

Fig. 1. Chain fragment in L$^{H/CF_3}$.

The temperature dependences of μ_{eff} for nitroxides L$^{R/CF_3}$ (R = H, Me, Et, Pr) are shown in Fig. 3. The μ_{eff} values at 300 K are close to the theoretical spin-only value for monoradicals (1.73 μ_B). As the temperature decreases, μ_{eff} first gradually decreases, and below 100 K, it sharply decreases, which is indicative of the predominance of antiferromagnetic exchange interactions between the nitroxide spins. The experimental $\mu_{eff}(T)$ dependences are well described by expression obtained by summation of contributions of the exchange-coupled dimers (spin Hamiltonian $H = -2JS_1S_2$) and monoradicals, the magnetic susceptibility χ of which obeys the Curie–Weiss law:

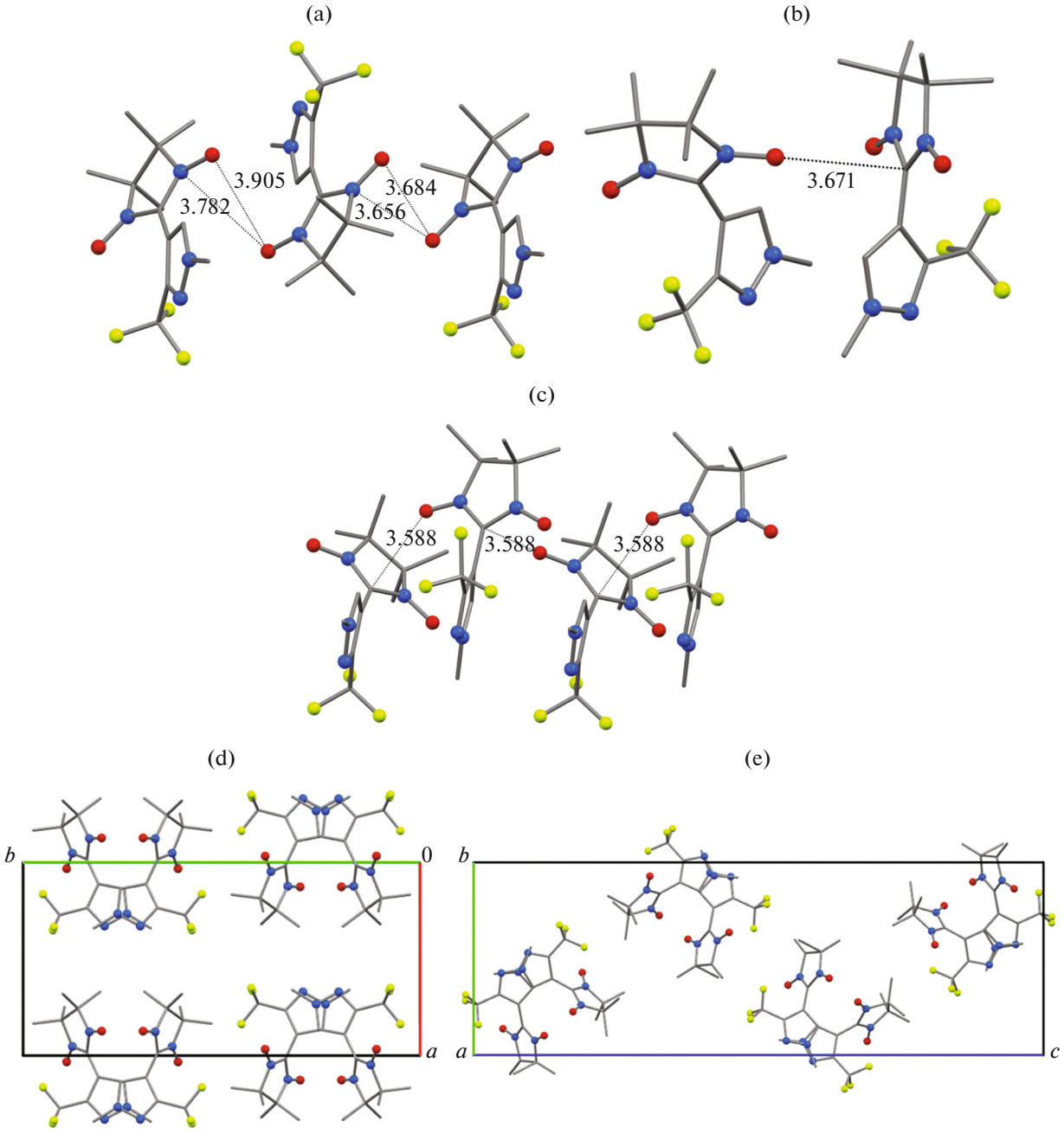

Fig. 2. Shortest contacts and packing of molecules in the L^{Me/CF_3}: polymorphs: (a) L^{Me/CF_3}-a; (b, c) L^{Me/CF_3}-b; (d, e) L^{Me/CF_3}-c.

$$\chi = (1-p)\chi_{dimer} + p\frac{g^2 0.375}{4(T-\theta)}, \quad \text{where} \quad \chi_{dimer} = \frac{3N\mu_B^2 g^2}{3kT}\frac{1}{3+e^{-2J/kT}}.$$

The optimal values of the exchange interaction parameters J, the fraction p, and the Weiss constant θ are -24.7 cm^{-1}, 3.4%, and 0 K (fixed) for L^{H/CF_3}; -12.0 cm^{-1}, 31%, and 0 K (fixed) for L^{Me/CF_3}; -13.9 cm^{-1}, 2.3%, and 0 K (fixed) for L^{Et/CF_3}; and -19.1 cm^{-1}, 90%, and 0.1 K for L^{Pr/CF_3}. The L^{Me/CF_3} sample is apparently a mixture of polymorphs, in one of which the nitroxides form exchange-coupled dimers (69%), while in the other one the exchange interactions between the radical spins are negligibly small (31%). Although in the case of L^{Pr/CF_3}, no polymorphs were

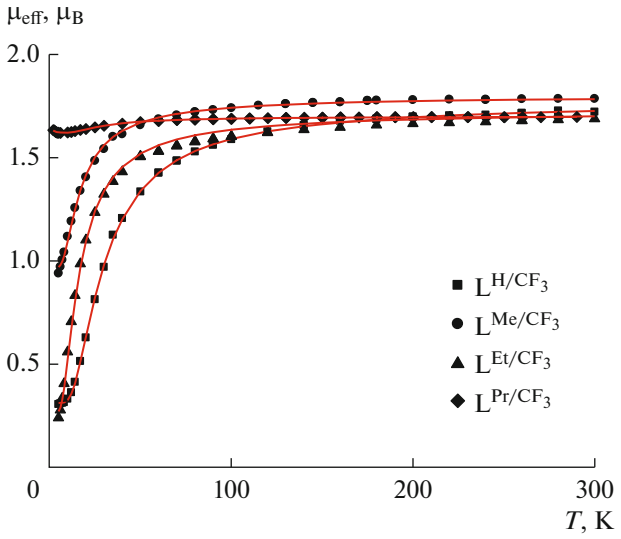

Fig. 3. Dependences $\mu_{eff}(T)$ for L^{R/CF_3} (R = H, Me, Et, Pr). Points are experimental values, continuous lines are theoretical curves.

found, the magnetochemical measurements showed that the sample probably contains an admixture of another phase L^{*Pr/CF_3} (10%) with a different crystal structure in which relatively strong antiferromagnetic interactions are present. The major part of the sample is a phase with weak ferromagnetic exchange interactions between the nitroxide spins, which is in line with the X-ray diffraction data for the crystal structure of L^{Pr/CF_3}.

Table 4. Stereochemical characteristics of nitroxides L^{R/CF_3}

Compound	N–O, Å	∠CN_2O_2-Pz, deg
L^{H/CF_3}	1.283(3), 1.290(3)	40.3
L^{Me/CF_3}-a	1.281(2), 1.270(2)	34.9
L^{Me/CF_3}-b	1.275(5), 1.284(5) 1.276(4), 1.267(4)	64.8 68.6
L^{Me/CF_3}-c	1.276(2), 1.281(2)	63.1
L^{Et/CF_3}	1.277(3), 1.287(3)	46.9
L^{Pr/CF_3}	1.273(4), 1.289(4)	50.0

The reaction of equimolar amounts of $Cu(Hfac)_2$ and L^{R/CF_3} (R = Me, Et, Pr) gave structurally similar polymer chain coordination compounds $[Cu(Hfac)_2L^{R/CF_3}]_n$ (**I**–**III**). As an example, Fig. 4 shows a fragment of the $[Cu(Hfac)_2L^{Me/CF_3}]_n$ chain. The paramagnetic ligands perform a bidentate bridging function by coordinating the O_{NO} atoms of the nitronyl nitroxide moiety to the neighboring $Cu(Hfac)_2$ moieties. This coordination mode is untypical of mono- and dialkylpyrazolyl-substituted nitroxides L^R and $L^{R/R'}$, but is implemented in the 3*d*-metal hexafluoroacetylacetonate complexes with alkyl-, isoxazolyl-, and phenyl-substituted nitronyl nitroxides [15–22].

The geometric characteristics of the centrosymmetric CuO_6 coordination units in complexes **I**–**III** are similar: the square planar environment of Cu(II) ions composed of four O_{Hfac} atoms is completed to a distorted octahedron by the O_{NO} atoms of two nitroxides. The Cu–O_{NO} distances are long: 2.344(2)–2.669(6) Å, and the ∠$CuO_{NO}N$ angles are in the 129.6(2)–152.0(2) range (Table 5).

The experimental $\mu_{eff}(T)$ dependences for complexes **I**–**III** are similar (Fig. 5). At 300 K, the μ_{eff} values are in the 2.7–2.8 μ_B range; as temperature decreases, they first gradually increase and, below 100 K, they sharply increase, which attests to the presence of ferromagnetic exchange interactions between the spins of the paramagnetic centers. This corresponds to the X-ray diffraction data, indicating axial coordination of nitroxide moieties by Cu^{2+} ions with distances of 2.3–2.4 Å. According to the results of theoretical studies [23, 24], this type of geometry of coordination units ensures the orthogonality of magnetic orbitals in the exchange clusters {>N–•O–Cu–O•–N<}. The experimental $\mu_{eff}(T)$ dependences were ana-

Table 5. Selected bond lengths (Å) and bond angles (deg) in polymer chain complexes **I**–**III**

Parameter	Complex					
	$[Cu(Hfac)_2(L^{Me/CF_3})]$ (**I**)		$[Cu(Hfac)_2(L^{Et/CF_3})]$ (**II**)		$[Cu(Hfac)_2(L^{Pr/CF_3})]$ (**III**)	
Cu–O_{NO}	2.496(2)	2.513(2)	2.344(2)	2.649(3)	2.368(6)	2.669(6)
Cu–O_{Hfac}	1.927(2) 1.931(2)	1.932(2) 1.946(2)	1.926(2)–1.937(2)		1.920(5)–1.951(5)	
∠CuON	152.0(2)	129.6(2)	131.2(2)	145.4(2)	132.7(5)	147.2(6)
N–O	1.278(3)	1.279(3)	1.290(3)	1.279(3)	1.292(7)	1.266(7)
∠CN_2O_2-Pz	37.4		38.1		39.6	

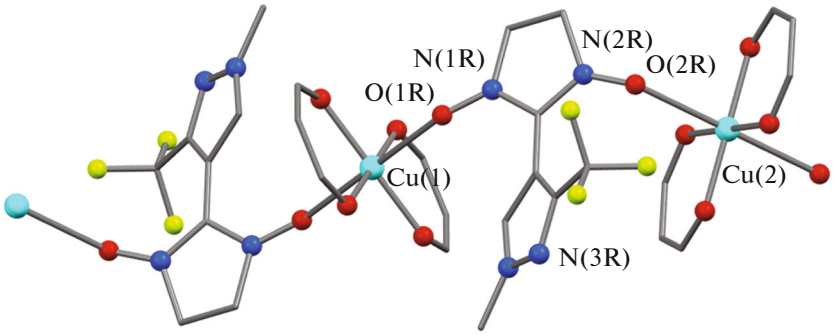

Fig. 4. Chain fragment in the structure of $[Cu(Hfac)_2L^{Me/CF_3}]_n$ at 295 K. Here and below, gray color shows the carbon skeleton, yellow-green is F, light blue is Cu, red is O, blue is N; H atoms, CF_3 groups of Hfac, and Me groups of the tetramethyl moiety are omitted.

lyzed using the expression for the magnetic susceptibility of ferromagnetically coupled chains [25] taking account of the interchain interactions zJ' in the molecular field approximation. The optimal exchange interaction parameters J and zJ' are 6.5 cm^{-1} and -0.28 cm^{-1} for complex **I**; 2.7 cm^{-1} and -0.22 cm^{-1} for complex **II**; and 2.4 cm^{-1} and -0.17 cm^{-1} for **III**. It is worth noting that a decrease in the interchain exchange interaction energy correlates with the increase in the size of the alkyl substituent in L^{R/CF_3}.

In the low temperature region, the dependences of the magnetization on the strength of the external magnetic field for complexes **I**–**III** are non-linear (Fig. 6). At 2 K in magnetic fields above 20 kOe, magnetization reaches a saturation level of ~2 μ_B, which attests to ferromagnetic spin ordering. The saturation magnetization is in good agreement with the theoretical value of 2.08 μ_B for two paramagnetic centers per formula unit:

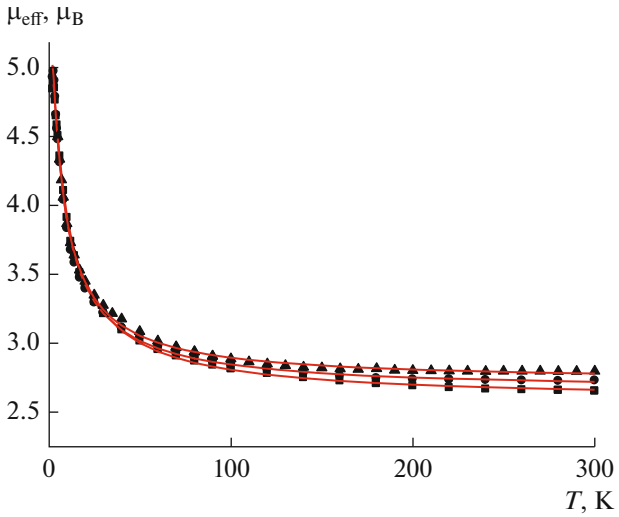

Fig. 5. Dependences $\mu_{eff}(T)$ for $[Cu(Hfac)_2L^{R/CF_3}]_n$, R = (■) Me, (●) Et, (▲) Pr. Points are experimental values, continuous lines are theoretical curves.

Cu(II) ion with the spin $S = 1/2$ at $g = 2.15$ and nitroxide with the spin $S = 1/2$ at $g = 2.00$. At 5 K, magnetization approaches saturation in magnetic fields above 40 kOe. Thus, the Curie temperature for complexes **I**–**III** can be estimated as $T_C \leq 3$ K.

For L^{Me/CF_3}, apart from the polymer chain complex, two polymorphs of the centrosymmetric molecular complex $[Cu(Hfac)_2\left(L^{Me/CF_3}\right)_2]$ were identified upon varying the reactant ratio. Synthetic difficulties precluded the isolation of pure phases in amounts sufficient for complete characterization. For this reason, magnetic properties were studied for only one polymorph, α-$[Cu(Hfac)_2\left(L^{Me/CF_3}\right)_2]$ (**IV**). The structures were solved for both α-polymorph and β-polymorph (**V**).

The molecules of α- and β-polymorphs differ in the Cu–O_{NO} bond lengths, which amount to 2.469(2) Å in **IV** and 2.317(2) Å in **V**, in the $\angle CN_2O_2$-Pz angles between the planes (Fig. 7), and in the intermolecular distances between uncoordinated O_{NO} atoms (Table 6). X-ray diffraction studies in the 300–120 K range demonstrated that the change in the Cu–O_{NO} bond lengths for the α-phase is insignificant (Δ = 0.041 Å), but the O_{NO}...O_{NO} intermolecular distances markedly (by 0.148 Å) decrease. In the β-phase on cooling to 120 K, the Cu–O_{NO} bond lengths are shortened by 0.262 Å, with one of the O_{Hfac}–Cu–O_{Hfac} axes being elongated (Δ = 0.250 Å); in other words, the direction of the elongated Jahn–Teller axis in the $\{CuO_6\}$ bipyramid changes. The shortening of the distances in the three-spin clusters {–•O–Cu–O•–} leads to switching of weak ferromagnetic exchange interactions to strong antiferromagnetic interactions.

Figure 8a shows the experimental $\mu_{eff}(T)$ dependence for the α-polymorph **IV**. The μ_{eff} value at 300 K amounting to 3.12 μ_B is consistent with the theoretical value of 3.0 μ_B for three non-interacting paramagnetic centers with $S = 1/2$ at $g = 2$. A decrease in the temperature below 100 K leads to a sharp decrease in μ_{eff}

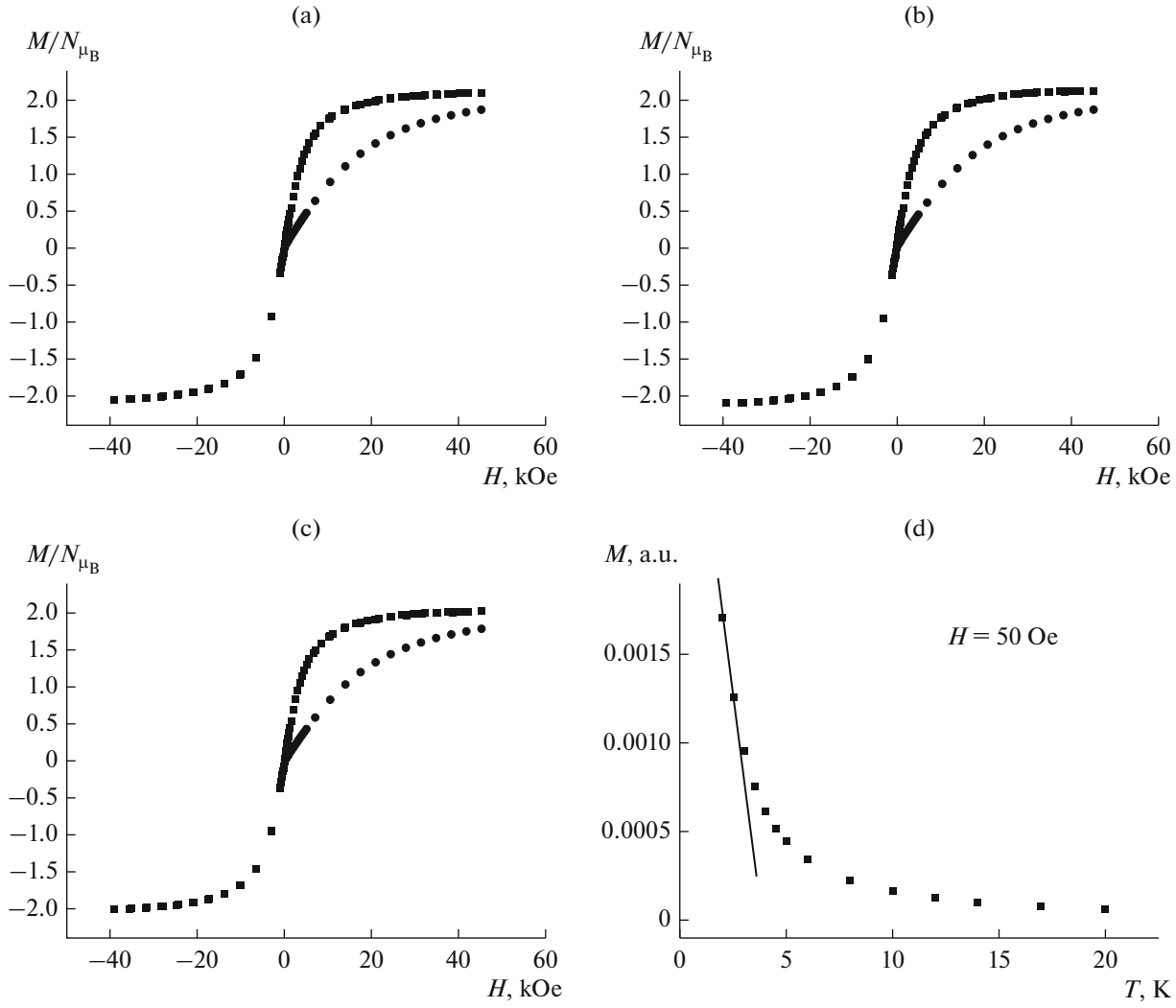

Fig. 6. Dependences $M(H)$ for $[Cu(Hfac)_2L^{R/CF_3}]_n$ (R = (a) Me, (b) Et, (c) Pr) at (■) 2 K and (●) 5 K. (d) Temperature dependence of the magnetization of $[Cu(Hfac)_2L^{Pr/CF_3}]_n$ in the field $H = 50$ Oe.

Table 6. Selected bond lengths (Å) and bond angles (deg) in complexes **IV** and **V**

Parameter	Complex					
	α-$[Cu(Hfac)_2(L^{Me/CF_3})_2]$ (**IV**)		β-$[Cu(Hfac)_2(L^{Me/CF_3})_2]$ (**V**)			
T, K	296	120	296	240	150	120
$Cu–O_{NO}$	2.469(1)	2.428(1)	2.316(2)	2.280(2)	2.175(2)	2.054(2)
N–O	1.286(2) 1.271(2)	1.287(2) 1.277(2)	1.292(3) 1.273(3)	1.288(2) 1.266(2)	1.300(2) 1.266(2)	1.303(3) 1.263(3)
$Cu–O_{Hfac}$	1.934(1) 1.940(1)	1.940(1) 1.940(1)	1.959(2) 1.975(2)	1.968(1) 1.992(1)	1.973(2), 2.073(2)	1.975(2) 2.225(2)
$\angle CN_2O_2$_Pz	39.2	39.6	27.0	25.5	24.7	25.3
–•O...O•–	3.706(2)	3.558(2)	4.707(4)	4.765(3)	4.786(3)	4.758(3)

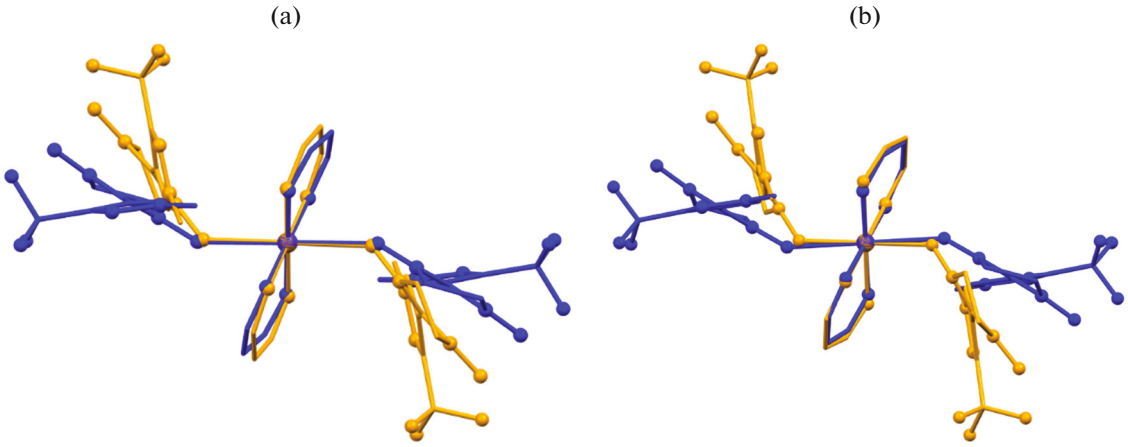

Fig. 7. Comparison of the molecular structures of α- and β-[Cu(Hfac)$_2$(L^{Me/CF_3})$_2$] at (a) 296 K and (b) 120 K (molecules of α-polymorph are in blue, β-polymorph—in yellow).

to reach 1.84 μ_B at 19 K; this corresponds to one paramagnetic center with $S = 1/2$ at $g = 2.12$, on average, and attests to the appearance of antiferromagnetic exchange interactions characteristic of equatorial coordination of nitroxides. Further decrease in μ_{eff} down to 1.57 μ_B at 5 K is attributable to the intermolecular exchange interactions between the paramagnetic centers.

Thus, in the solid phases of both polymorphs **IV** and **V**, thermally induced phase transitions take place; according to magnetochemical measurements, in the case of the α-phase, the transition occurs in the temperature range of 100–20 K, while for the β-phase, the main structural changes occur in the temperature range of 250–120 K. For comparison, Fig. 8b shows the variation of the fraction of the high-temperature phase on lowering the temperature for **IV** and **V** calculated from experimental data. The fraction ω of clusters in which the structural transition has taken place was estimated for the α-polymorph from analysis of the $\mu_{eff}(T)$ dependence using the expression $\mu_{eff}^2 = (1 - \omega)(\mu_{LT})^2 + \omega(\mu_{HT})^2$, where $\mu_{LT} = 1.84$ μ_B, $\mu_{HT} = 3.12$ μ_B are the μ_{eff} values for the low-spin and high-spin polymorphs, respectively. In the case of β-polymorph, the decrease in the fraction of high-spin clusters was estimated from the relative change in the Cu–O_{NO} distances with the assumption that the Cu–O_{NO} distance of 2.469(1) Å (as in the α-phase) corresponds to 100% content of high-spin clusters, while 1.99 Å

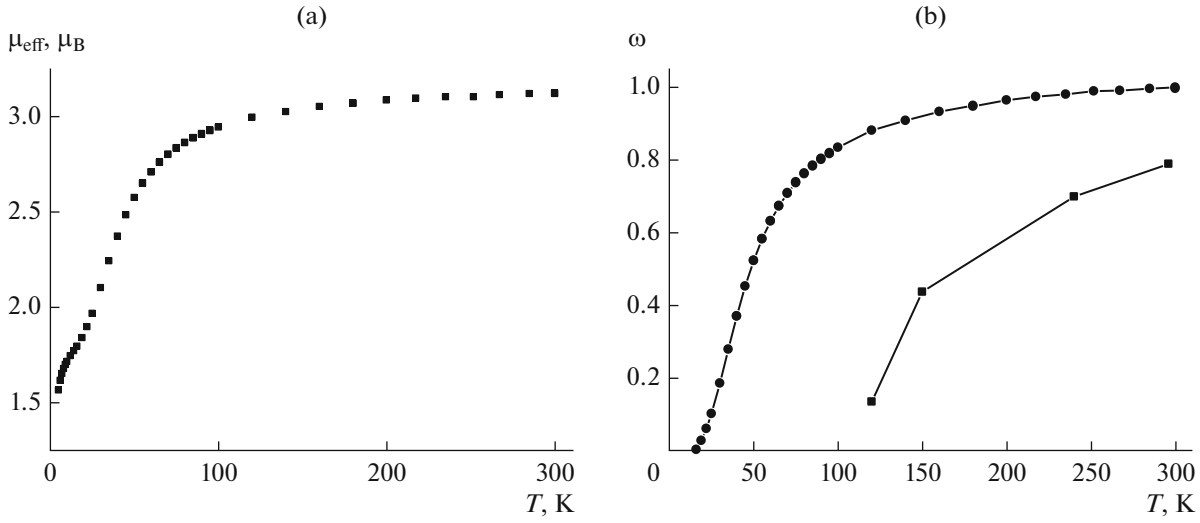

Fig. 8. (a) Dependence $\mu_{eff}(T)$ for α-[Cu(Hfac)$_2$(L^{Me/CF_3})$_2$] and (b) temperature dependences of the fraction of the high-temperature phase for (●) α- and (■) β-polymorphs of [Cu(Hfac)$_2$(L^{Me/CF_3})$_2$].

corresponds to 100% low-spin clusters. Actually, polymorphs **IV** and **V** are new examples of molecular heterospin complexes capable of undergoing thermally induced magnetic structural single-crystal-to-single-crystal transformations.

Thus, as a result of present study, CF_3-substituted spin-labeled pyrazoles L^{R/CF_3} were synthesized and characterized. It was established that the introduction of the CF_3 group into the pyrazole ring decreases the donor ability of the pyrazole nitrogen atom, which leads to coordination of only the O_{NO} atoms of the nitroxide paramagnetic moiety. The bidentate bridging coordination of the paramagnetic ligand gives rise to polymer chain complexes $[Cu(Hfac)_2L^{R/CF_3}]_n$, which exhibited ferromagnetic ordering at temperature below 5 K. The monodentate coordination of nitronyl nitroxide leads to the mononuclear molecular complex $[Cu(Hfac)_2\left(L^{Me/CF_3}\right)_2]$, which exists as two polymorphs, both able to undergo thermally induced magneto-structural phase transitions.

FUNDING

This study was supported by the Russian Science Foundation (grant no. 18-13-00380).

CONFLICT OF INTEREST

The authors declare that they have no conflicts of interest.

REFERENCES

1. Ovcharenko, V.I., Maryunina, K.Y., Fokin, S.V., et al., *Russ. Chem. Bull.*, 2004, vol. 53, no. 11, p. 2406.
2. Ovcharenko, V., in *Stable Radicals*: *Fundamentals and Applied Aspects of Odd-Electron Compounds*, Hicks, R., Ed., Chichester: Wiley, 2010, p. 461.
3. Ovcharenko, V. and Bagryanskaya, E., in *Spin-Crossover Materials*: *Properties and Applications*, Halcrow, M.A., Ed., Oxford: Wiley, 2013, p. 239.
4. Ovcharenko, V.I., Romanenko, G.V., Maryunina, K.Y., et al., *Inorg. Chem.*, 2008, vol. 47, no. 20, p. 9537.
5. Romanenko, G.V., Maryunina, K.Y., Bogomyakov, A.S., et al., *Inorg. Chem.*, 2011, vol. 50, no. 14, p. 6597.
6. Romanenko, G.V., Fokin, S.V., Chubakova, E.T., et al., *J. Struct. Chem.*, 2022, vol. 63, no. 1, p. 87.
7. Ovcharenko, V.I., Fokin, S.V., Kostina, E.T., et al., *Inorg. Chem.*, 2012, vol. 51, no. 22, p. 12188.
8. Ovcharenko, V., Fokin, S., Chubakova, E., et al., *Inorg. Chem.*, 2016, vol. 55, no. 12, p. 5853.
9. Fokin, S.V., Kostina, E.T., Tret'yakov, E.V., et al., *Russ. Chem. Bull.*, 2013, vol. 62, no. 3, p. 661.
10. Naumov, P., Chizhik, S., Panda, M.K., et al., *Chem. Rev.*, 2015, vol. 115, no. 22, p. 12440.
11. Ovcharenko, V.I., Fokin, S.V., Romanenko, G.V., et al., *Russ. Chem. Bull.*, 1999, vol. 48, no. 8, p. 1519.
12. Gallagher, M.G., Jamieson, C.C., Lyons, A.J., et al., US Patent 2009/0131455A1 USA, 2009, p. 18.
13. Sheldrick, G.M., *Acta Crystallogr., Sect. C: Cryst. Chem.*, 2015, vol. 71, no. 1, p. 3.
14. Tretyakov, E.V. and Ovcharenko, V.I., *Russ. Chem. Rev.*, 2009, vol. 78, no. 11, p. 971.
15. Caneschi, A., Gatteschi, D., Laugier, J., and Rey, P., *J. Am. Chem. Soc.*, 1987, vol. 109, no. 7, p. 2191.
16. Ressouche, E., Boucherle, J.X., Gillon, B., et al., *J. Am. Chem. Soc.*, 1993, vol. 115, no. 9, p. 3610.
17. Onguchi, T., Fujita, W., Yamaguchi, A., et al., *Mol. Cryst. Liq. Cryst.*, 1997, vol. 296, no. 1, p. 281.
18. Caneschi, A., Gatteschi, D., Sessoli, R., et al., *J. Mater. Chem.*, 1992, vol. 2, no. 12, p. 1283.
19. Caneschi, A., Gatteschi, D., Renard, J.P., et al., *Inorg. Chem.*, 1989, vol. 28, no. 17, p. 3314.
20. Koreneva, O.V., Romanenko, G.V., Shvedenkov, Y.G., et al., *Polyhedron*, 2003, vol. 22, nos. 14–17, p. 2487.
21. Fokin, S.V., Tolstikov, S.E., Tretyakov, E.V., et al., *Russ. Chem. Bull.*, 2011, vol. 60, no. 12, p. 2470.
22. Sherstobitova, T., Maryunina, K., Tolstikov, S., et al., *ACS Omega*, vol. 4, no. 17, p. 17160.
23. De Panthou, F.L., Luneau, D., Musin, R., et al., *Inorg. Chem.*, 1996, vol. 35, no. 12, p. 3484.
24. Musin, R.N., Schastnev, P.V., and Malinovskaya, S.A., *Inorg. Chem.*, 1992, vol. 31, no. 20, p. 4118.
25. Baker, G.A., Rushbrooke, G.S., and Gilbert, H.E., *Phys. Rev.*, 1964, vol. 135, no. 5, p. A1272.

Translated by Z. Svitanko